Eleventh International Conference on CFD in the Minerals and Process Industries
CSIRO, Melbourne, Australia
7-9 December 2015

BED EXPANSION BEHAVIOUR IN A BINARY SOLID-LIQUID FLUIDISED BED WITH DIFFERENT INITIAL SOLID LOADING- CFD SIMULATION AND VALIDATION

Md. Shakhaoath KHAN[1], Subhasish MITRA[1], Ifsana KARIM[1], Swapnil V. GHATAGE[1], Zhengbiao PENG[1], Elham DOROODCHI[1], Behdad MOGHTADERI[1], Jyeshtharaj B. JOSHI [2] and Geoffrey M. EVANS[1*]

[1] Discipline of Chemical Engineering, University of Newcastle, Callaghan, NSW 2308, AUSTRALIA
[2] Homi Bhabha National Institute, Anushaktinagar, Mumbai 400 094, INDIA
*Corresponding author, E-mail address: Geoffrey.Evans@newcastle.edu.au

ABSTRACT

Expansion behaviour of a binary solid-liquid fluidised bed (SLFB) system with different initial mass of solids was studied both experimentally and numerically. Three different sizes (3, 5 & 8 mm diameter) of borosilicate glass beads of equal density (2230 kgm^{-3}) were used as fluidised particles. Three different combinations of particle size pairs of both equal and unequal mass ratios were used using a constant liquid (water) superficial velocity of 0.17 ms^{-1} in all the cases. Numerically, a two dimensional Eulerian-Eulerian (E-E) CFD model incorporating kinetic theory of granular flow (KTGF) was developed to predict the bed expansion behaviour. It was observed that complete bed segregation occurred when the difference between the solid particle diameters was higher while lower difference in particle diameters led to partial bed segregation. The CFD model also predicted these behaviours which were in good agreement with the experimental data.

Keywords: CFD; SLFB; binary mixtures; solids mass.

NOMENCLATURE

$C_{D\infty}$	drag coefficient under terminal rise conditions, -
$C_{fr,ss}$	coefficient of friction between solids, -
d_S	diameter of solid, m
D_c	column diameter, m
e_{SS}	solid-solid interaction restitution coefficient, -
e_{SW}	solid-wall interaction restitution coefficient, -
F_{Di}	momentum exchange term, N
g	gravitational acceleration, ms^{-2}
$g_{0,ss}$	radial distribution function, -
h	axial location, m
k_L	turbulent kinetic energy, m^2s^{-2}
M_r	mass ratio of larger to smaller solids, -
M_S	total mass of binary solids, kg
n	Richardson-Zaki index, -
P	static pressure, Pa
P_S	solid pressure, Pa
P_{kL}	production of turbulent kinetic energy, m^2s^{-3}
Re_{Si}	solid particle Reynolds number, -
$v_{S\infty i}$	solid terminal settling velocity, ms^{-1}
v_S	solid velocity, ms^{-1}
v_L	liquid superficial velocity, ms^{-1}
Greek letters	
μ_L	viscosity of liquid, $kgm^{-1}s^{-1}$
μ_S	solid viscosity, $kgm^{-1}s^{-1}$
μ_T	turbulent viscosity, $kgm^{-1}s^{-1}$
$\mu_{eff,s}$	effective viscosity of solid, $kgm^{-1}s^{-1}$
$\mu_{eff,L}$	effective viscosity of liquid, $kgm^{-1}s^{-1}$
λ_S	bulk viscosity of solid, $kgm^{-1}s^{-1}$
ρ_S	solid density, kgm^{-3}
ρ_L	liquid density, kgm^{-3}
ϵ_S	volume fraction of solid, -
ϵ_L	liquid voidage, -
ε_L	energy dissipation rate per unit mass, m^2s^{-3}
β_{SL}	liquid-solid momentum exchange force, $kgm^{-2}s^{-2}$
β_{SS}	solid-solid momentum exchange force, $kgm^{-2}s^{-2}$
ϕ	shape factor (equal to 1 for spherical solids), -

INTRODUCTION

Solid-liquid fluidization is the suspension of dispersed phase (solid) by a continuous moving fluid (liquid). SLFBs are extensively used in a variety of engineering applications including particle classification by size and density in mineral processing industries, backwashing of granular filters, mineral washing/leaching, ion exchange, adsorption, crystallization and many more. The computational modelling of a SLFB is challenging due to their multifaceted flow behaviour and interactions between the phases. The numerical analysis which aids in design and performance of SLFB systems is indeed beneficial. It is possible due to advances in computational resources and development of improved physical models for multiphase interactions. Specifically, CFD simulations can be used to provide comprehensive details such as spatial and temporal distribution of local volume fractions of liquid and solids, the intermixing heights of the separate phases particularly in the areas where quantification is either tedious or difficult. Many CFD studies on SLFB systems investigating the various flow regimes and related parameters are available in published literature. However, CFD studies related to binary SLFB with two different solid species are scarce. These solid species differ in size and/or density. Table 1 briefly summarizes the reported CFD studies on the binary SLFB systems. Although these studies addressed the hydrodynamics of SLFBs in general, no studies in particular focus on the mixing and segregation phenomena in SLFB systems and more importantly, the effect of solid mass ratio on the bed expansion behaviour. The present study is concerned with developing a CFD model using Ansys Fluent CFD commercial code (version 15.0) to simulate fluidisation of binary mixture of particles with different sizes. The model is used to demonstrate the influence of the solid mass on the bed expansion in terms of variation in total bed height. The CFD-generated data are compared with the experimental data of Khan et al. (2015).

Authors	CFD code	SLFB size ($D_c \times h$)	Drag model	e_{ss}	e_{sw}	Solids B.C. at wall	Liquid turbulence	Radial distribution function	Solid	Liquid	Remarks
Syamlal and O'Brien (1988)	multi-particle numerical model	50×300	Syamlal and O'Brien (1988)	NS		NS	NS	NS	0.163mm GB & 0.775mm HC	Water	1
Roy and Dudukovic (2001)	Fluent	152.4×2133.6	Wen and Yu (1966)	0.98	0.98	Jackson condition	k-ε model	NS	2.5 mm GB	Water	2
Cheng and Zhu (2005)	Fluent 4.5.6	76×3000	Wen and Yu (1966)	1.0	0.99	Jackson condition	k-ε model	NS	0.51mm and 2.5 mm GB	Water	3
Doroodchi et al. (2005)	CFX 5.6	50×1300 (Inclined)	Richardson and Zaki (1954)	NA	NA	Free slip	laminar	NA	0.08mm and 0.137 mm GB	Water	4
Lettieri et al. (2006)	CFX 4.4	30×1250	Ihne et al. (1972) & Gidaspow (1994)	0.90	NS	No slip	NS	Ding and Gidaspow (1990)	1.7 mm lead shot	Water	5
Cornelissen et al. (2007)	Fluent 6.1.22	127×1100	Wen and Yu (1966) & Gidaspow (1994)	0.90	0.90	No slip	Laminar	Ding and Gidaspow (1990)	1.13mm GB	Water	6
Reddy and Joshi (2008)	Fluent 6.2	127×247.3 127×249.5 127×245.4	Joshi (1983) & Pandit and Joshi (1998)	0.9	0.9	No slip	k-ε model	Ding and Gidaspow (1990)	24.5mm	Water	7
Reddy and Joshi (2009)	Fluent 6.2	100×1200 100×800 50×800 50×400	Joshi (1983) & Pandit and Joshi (1998)	0.9	0.9	No slip	k-ε model	Ding and Gidaspow (1990)	3, 1.03, 3.95mm GB & 0.8mm IER	Glycerine solution, Water	7
Fan et al. 2010	Fluent 6.3	50×2000	Gidaspow (1994) & Syamlal-O'Brien symmetric (1988)	0.9	0.9	No slip	laminar	NS	1mm coloured by density	Water	8
Davarnejad et al. (2014)	Fluent 6.3.26	60×1000	Gidaspow (1994) & Syamlal-O'Brien symmetric (1988)	0.9	0.9	Jackson condition	laminar	Ogawa and Umemura (1980)	1.396 mm Pet and 2.465mm GB	Water	9

B.C.: Boundary condition; NA: Not applicable; NS: Not specified; PET: polyethylene terephthalate resin; GB: Glass beads; HC: Hollow char; IER: Ion exchange resin

Remarks: (1) studied segregation in a binary SLFB using a multi-particle numerical model and obtained semi-quantitative agreement with experimental data without any tuning of adjustable parameters, a comprehensive representation of the solids distribution in the bed can be seen that shows radial segregation patterns; (2) analysed a CFD simulation providing solids velocity profiles and holdup as well as solids and liquid RTDs and obtained qualitative results with experiments; (3) investigated the influence of column diameter (varied from 76 to 600 mm) on the radial velocity, turbulent kinetic energy and granular temperature of solid particles by carried out CFD simulations in circulating SLFB; (4) investigate the influence of inclined plates on the expansion behaviour of the mono-dispersed and binary suspensions in SLFB and validated against their experimental data; (5) simulate SLFB of lead particles in slugging mode using granular kinetic theory and with the increase of the superficial liquid velocity (from 80 to 300 mm/s) the gradual development of the slugging regime can be seen from their simulation; (6) investigated the effects of mesh size, time step and convergence criteria on the bed expansion by simulating SLFB having 1.13 mm glass particles in the range of superficial liquid velocities from 8.5 to 110 mm/s; (7) investigates mono-component phase pressure drop and drag coefficient in the fixed as well as expanded beds in the creeping, transition and turbulent flow regimes, due to the wall friction in the creeping flow a rise of pressure drop was found and also due to the channelling near the wall in turbulent regime the pressure drop was found decreases; (8) predicts the expansion and segregation behaviour of a binary SLFB for particles in the same narrow (1.00-1.18 mm) size range, with different densities (1600 and 1900 kg/m^3) fluidised by water; (9) simulated a binary SLFB by adopting the multi fluid Eulerian CFD model with granular flow extension in the laminar flow, temperature among 20-25°C and below atmospheric pressure, and compared CFD predicted bed voidage with the different averaging approaches and experimental data form the literature and found good agreement.

Table 1: Previous computational fluid dynamics studies on binary SLFB

MODEL DESCRIPTION

A 2D CFD model based on the E-E approach (two-fluid model) was adopted where both phases (solid and liquid) are regarded as interpenetrating continua. Each phase has its own set of conservation equations of mass and momentum, coupled with suitable phase interaction terms. The general purpose finite volume method based solver ANSYS Fluent (ver: 15.0) was used to solve these governing equations. The standard continuity and momentum equations were applied to the liquid and the solid phases. Two solid phases having volume fraction of ϵ_{S1} and ϵ_{S2} were considered to model the binary mixture. The mass conservation is ensured by putting the constraint on sum total of the individual phase fraction equal to one. The SIMPLE algorithm provides a methodology for solving the pressure field by forming pressure equation by manipulating the momentum and continuity equations. Performance of the multiphase CFD model critically depends on the adequate treatment of the momentum exchange between the phases to account for the presence of various forces. Drag force is often considered as the key parameter which governs the overall hydrodynamics compared to other forces such as lift force and virtual mass force which are often ignored (Cheng and Zhu, 2005; Cornelissen et al., 2007). Considering only the effect of drag force, the momentum exchange term, F_D, for each pair of phases (solid1/liquid and solid2/liquid) was therefore calculated as:

$$\begin{aligned} F_{D1} &= \beta_{S1L}\left(\overrightarrow{v_{S1}} - \overrightarrow{v_L}\right) \\ F_{D2} &= \beta_{S2L}\left(\overrightarrow{v_{S2}} - \overrightarrow{v_L}\right) \end{aligned} \quad , \qquad (1)$$

Description of momentum exchange coefficients

Two different interphase momentum exchange parameters were used: solid–liquid (β_{SL}) and solid–solid (β_{SS}). The interaction parameters account for the momentum transfer between a pair of phases due to relative velocity.

Solid–liquid momentum exchange coefficients

The Gidaspow (1994) drag model was used to compute β_{SL} which is a combination of Ergun (1952) equation and Wen and Yu (1966) model. For high solid concentrations, $\epsilon_L \leq 0.8$ (Ergun, 1952) these momentum exchange parameters are given as:

$$\begin{aligned} \beta_{S1L} &= \frac{150\mu_L\left(1-\epsilon_L\right)^2}{\epsilon_L\left(d_{S1}\phi\right)^2} + \frac{1.75\rho_L\left(\left|\overrightarrow{v_{S1}} - \overrightarrow{v_L}\right|\right)\left(1-\epsilon_L\right)}{d_{S1}\phi} \\ \beta_{S2L} &= \frac{150\mu_L\left(1-\epsilon_L\right)^2}{\epsilon_L\left(d_{S2}\phi\right)^2} + \frac{1.75\rho_L\left(\left|\overrightarrow{v_{S2}} - \overrightarrow{v_L}\right|\right)\left(1-\epsilon_L\right)}{d_{S2}\phi} \end{aligned} . \qquad (2)$$

For very low solid concentrations, $\epsilon_L > 0.8$ (Wen and Yu, 1966), these momentum exchange parameters are given as:

$$\begin{aligned} \beta_{S1L} &= \frac{3}{4}C_{D1}\frac{\epsilon_L\left|\overrightarrow{v_{S1}} - \overrightarrow{v_L}\right|\rho_L\left(1-\epsilon_L\right)}{d_{S1}}f\left(\epsilon_L\right) \\ \beta_{S2L} &= \frac{3}{4}C_{D2}\frac{\epsilon_L\left|\overrightarrow{v_{S2}} - \overrightarrow{v_L}\right|\rho_L\left(1-\epsilon_L\right)}{d_{S2}}f\left(\epsilon_L\right) \end{aligned} , \qquad (3)$$

where $f\left(\epsilon_L\right) = \epsilon_L^{-2.65}$ (Gidaspow, 1994).

The particle drag coefficient, C in Eq.(3) is given by:

$$\begin{aligned} C_{D1} &= \max\left(\frac{24}{Re_{S1}}\left(1+0.15Re_{S1}^{0.687}\right), 0.44\right) \\ C_{D2} &= \max\left(\frac{24}{Re_{S2}}\left(1+0.15Re_{S2}^{0.687}\right), 0.44\right) \end{aligned} , \qquad (4)$$

where the particle Reynolds number, Re_S, defined as:

$$\begin{aligned} Re_{S1} &= \epsilon_L\left(\rho_L\left|\overrightarrow{v_{S1}} - \overrightarrow{v_L}\right|d_{S1}/\mu_L\right) \\ Re_{S2} &= \epsilon_L\left(\rho_L\left|\overrightarrow{v_{S2}} - \overrightarrow{v_L}\right|d_{S2}/\mu_L\right) \end{aligned} . \qquad (5)$$

Solid–solid momentum exchange coefficients

To model solid-solid interactions, the solid-solid momentum exchange coefficient suggested by Syamlal and O'Brien (1988) was used:

$$\beta_{SS} = \frac{3\left(1+e_{ss}\right)\left(\frac{\pi}{2}+C_{fr,ss}\frac{\pi^2}{8}\right)\left(1-\epsilon_L\right)\rho_{susp}\,\epsilon_L\,\rho_L d_{s,avg}^2 g_{0,ss}}{2\pi d_{s,avg}^3\left(\rho_{susp}+\rho_L\right)}\left|\overrightarrow{v_{s1}} - \overrightarrow{v_{s2}}\right| \qquad (6)$$

where $g_{0,ss}$ is the radial distribution coefficient.
This coefficient is a function of solid volume fraction and accounts for the probability of collisions between the solid particles when the solid granular phase becomes dense (Ogawa et al., 1980).

$$g_0 = \left[1-\left(\frac{\epsilon_S}{\epsilon_{S,max}}\right)^{1/3}\right]^{-1} . \qquad (7)$$

Kinetic theory of granular flow (KTGF)

Kinetic theory of granular flow model was used as closure for the solid phase which considers the conservation of solid fluctuation energy. This theory is an analogy following Chapman and Cowling (1970) and provides the dependency of the rheological material properties (granular viscosity, granular pressure, etc.) on the volume fraction of solids and on the solids fluctuating velocity due to collisions among solids. With this understanding, the actual velocity of solid, $\overrightarrow{V_S}$ can be decomposed into a local mean velocity $\overrightarrow{v_S}$ and a random fluctuating velocity, $\overrightarrow{C_S}$ as follows:

$$\overrightarrow{V_S} = \overrightarrow{v_S} + \overrightarrow{C_S} . \qquad (8)$$

The random fluctuating velocity is associated with the granular temperature, θ, and for an assembly of solid particles, it is defined as:

$$\theta = \frac{1}{3}\left\{\overrightarrow{C_S}\cdot\overrightarrow{C_S}\right\} , \qquad (9)$$

where the brackets symbolize ensemble averaging. For detail description of the KTGF model, reader can refer to the Fluent theory guide (2013).

Turbulence modelling

The k-ε approach based on modelled equations for the turbulent kinetic energy (k_L) and turbulent dissipation rate (ε_L) to model the system turbulence has been employed to the present study. The standard k-ε model has five empirical model constants C_μ, $C_{\varepsilon 1}$, $C_{\varepsilon 2}$, σ_k and σ_ε in its formulation and their values are 0.09, 1.44, 1.92, 1.0 and 1.3, respectively. These values have been determined from experimentations with air and water for fundamental turbulent shear flows together with homogeneous shear

flows and decaying isotropic grid turbulence (Fluent theory guide, 2013). They have been found to work fairly well for SLFB (Reddy and Joshi, 2007; Reddy and Joshi, 2009). The mathematical expression for k_L and ε_L are given below:

$$\frac{\partial(\epsilon_L \rho_L k_L)}{\partial t} + \frac{\vec{v}_L \partial(\epsilon_L \rho_L k_L)}{\partial x_i} = \nabla\left(\epsilon_L\left(\mu_L + \frac{\mu_T}{\sigma_{kL}}\right)\nabla k_L\right) + \epsilon_L \rho_L (P_{kL} - \varepsilon_L) \quad , (10)$$

$$\frac{\partial(\epsilon_L \rho_L \varepsilon_L)}{\partial t} + \frac{\vec{v}_L \partial(\epsilon_L \rho_L \varepsilon_L)}{\partial x_i} = \nabla\left(\epsilon_L\left(\mu_L + \frac{\mu_T}{\sigma_{\varepsilon L}}\right)\nabla \varepsilon_L\right) + \epsilon_L \rho_L \frac{\varepsilon_L}{k_L}(C_{\varepsilon 1} P_{kL} - C_{\varepsilon 2}\varepsilon_L) \quad , (11)$$

where, the turbulent viscosity of the liquid phase is obtained by the k-ε model:

$$\mu_T = C_\mu \rho_L \left(\frac{k_L^2}{\varepsilon_L}\right). \quad (12)$$

Computational geometry and boundary conditions

A 2D rectangular domain (0.05m x 0.7m) comprising 30,000 structured cells were used for computational purpose. Uniform liquid superficial velocity at the inlet, constant pressure at the column outlet and no slip boundary condition was specified at the wall. Different setup parameters used in the CFD model are summarized in Table 2.

Parameters	Numerical Value	Unit
Reactor size	0.05×0.7	m
Grid number	50×600	-
Convergence criteria	10^{-3}	-
Maximum iterations	100	-
Time step	0.0005	s
Discretization method	Second order upwind	
Model precision	Double	
Packing limit, $\epsilon_{s,max}$	0.6	-
ess, esw	0.9	-
Operating pressure	1.013×10^5	Pa
Gravitational acceleration	9.81	ms^{-2}
Granular viscosity	Gidaspow (1994)	
Granular bulk viscosity	Lun et al. (1984)	
Solid pressure	Lun et al. (1984)	
Radial distribution	Lun et al. (1984)	

Table 2: Geometry, initial, boundary and operating parameters used in numerical analysis.

RESULTS

The predicted overall bed expansion values after 100 s of CFD simulations of three different binary solid mixtures with different solid initial mass (Table 3) at the same liquid superficial velocities V_L=0.17 ms^{-1} were compared (Figure 1) with the experimental data of Khan et al. (2015). Figures 2-7 display experimental images of different mixture of binary solids (equal and unequal mass combination) together with corresponding CFD predicted volume fractions contour profile of water and glass beads. The axial distributions of solids concentration are also depicted which are the area weighted averaged values at time step 100 s.

Mass of small particles (kg)	Mass of large particles (kg)	Total mass of particles (kg)	Mass Ratio M_r (-)
0.24	0.04	0.28	0.17
0.24	0.08	0.32	0.33
0.24	0.12	0.36	0.50
0.24	0.16	0.40	0.67
0.24	0.20	0.44	0.83
0.04	0.04	0.08	1.00
0.08	0.08	0.16	1.00
0.12	0.12	0.24	1.00
0.16	0.16	0.32	1.00
0.20	0.20	0.40	1.00
0.24	0.24	0.48	1.00
0.20	0.24	0.44	1.20
0.16	0.24	0.40	1.50
0.12	0.24	0.36	2.00
0.08	0.24	0.32	3.00
0.04	0.24	0.28	6.00

Table 3: Initial mass of three binary solid mixtures (3 & 8 mm, 3 & 5mm and 5 & 8 mm).

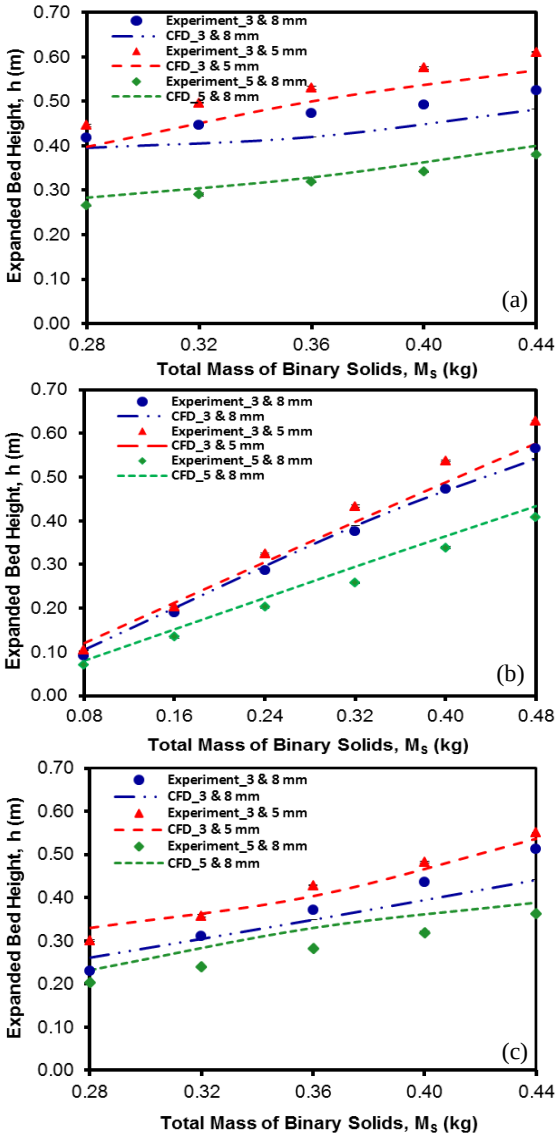

Figure 1: Experimental-CFD SLFB bed expansion varying total solid initial masses: (a) M_r = 0.17 to 0.83, (b) M_r = 1.0, (c) M_r = 1.2 to 6.0.

Figure 1 represents comparison of fluidised bed expansions between experiments and CFD predicted data

for three different binary solid particles mixture involving different initial mass of solids (equal & unequal mass combinations). In Figure 1a the bed expands within the range of 0.27 to 0.61 m in experiments whereas CFD predicts 0.28 to 0.57 m however 3-12% deviation can be observed in the simulation results. Experimentally SLFB was found expanded from 0.07 to 0.63 m in Figure 1b though CFD results shows 0.08 to 0.58 m of bed expansion having 3-13% deviations from experimental data. Figure 1c displays SLFB expanded between the ranges 0.20 to 0.55 m whereas CFD predicts a range 0.23 to 0.53 m and 0.1-16% of deviation can be seen from CFD results.

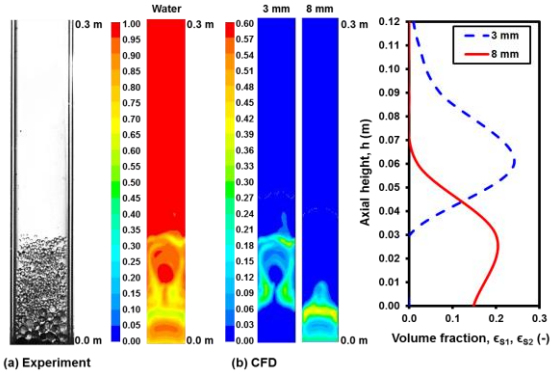

Figure 2: Binary SLFB of 3 mm (40gm) and 8 mm (40gm) glass beads: (a) experiment, (b) CFD contours of liquid and solid concentration.

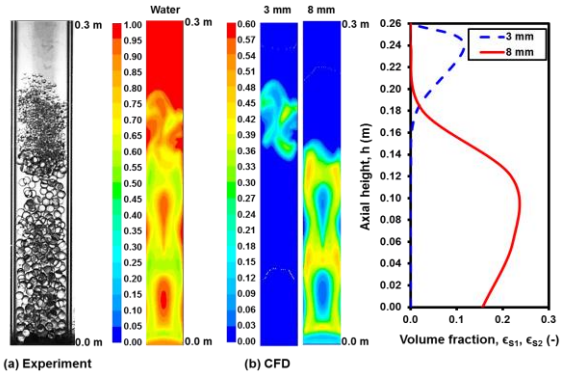

Figure 3: Binary SLFB of 3 mm (40gm) and 8 mm (240gm) glass beads: (a) experiment, (b) CFD contours of liquid and solid concentration.

Figures 2 & 3 represent binary SLFB of 3 & 8 mm glass beads for equal and unequal mass ratio of solids respectively. A complete segregation of the bed was achieved experimentally for both cases. An interface was clearly observed between two mono-component zones. Comparable profiles of liquid and liquid volume fractions with two segregated zones (8 mm at the bottom & 3 mm at the top) were also observed in the CFD simulation.

Figures 4 & 5 shows binary SLFB of 5 & 8 mm glass beads. It can be seen that the fluidized bed was partially segregated or partially intermixed (two segregated zone containing 8 mm solids at the bottom and 5 mm at the top respectively and a mixed zone between two mono-component zones) for both equal and unequal mass combinations of binary solid particles. CFD over predicts the overall bed expansion where a positive deviation can be observed in Figure 4. However two mono-component zones and an intermixing zone clearly observed in the simulation results for unequal mass combinations.

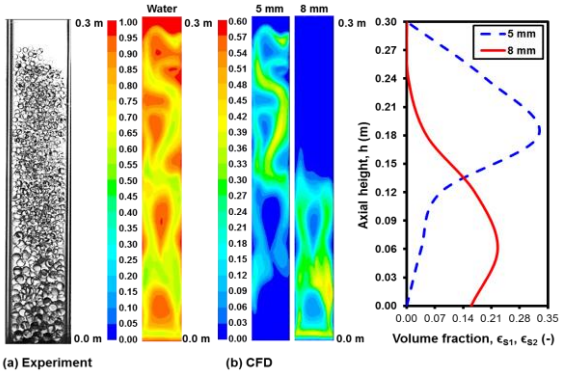

Figure 4: Binary SLFB of 5 mm (160 gm) and 8 mm (160 gm) glass beads: (a) experiment, (b) CFD contours of liquid and solid concentration.

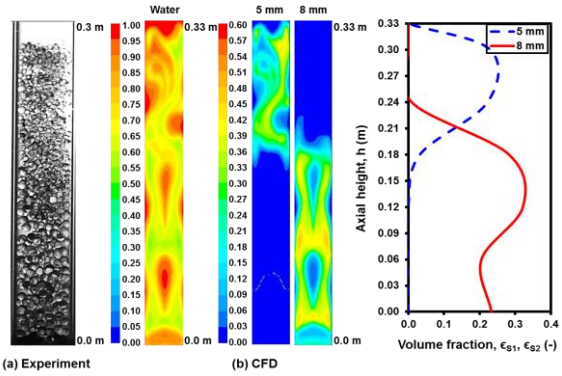

Figure 5: Binary SLFB of 5 mm (120 gm) and 8 mm (240 gm) glass beads: (a) experiment, (b) CFD contours of liquid and solid concentration.

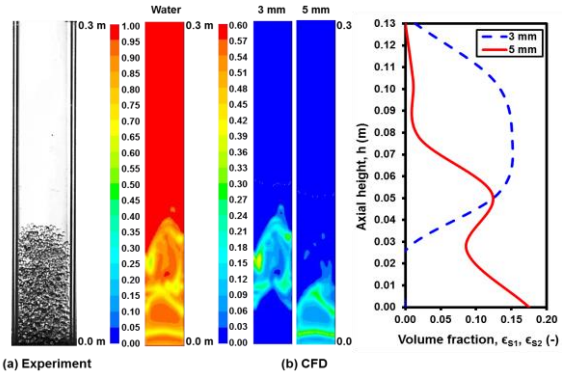

Figure 6: Binary SLFB of 3 mm (40 gm) and 5 mm (40 gm) glass beads: (a) experiment, (b) CFD contours of liquid and solid concentration.

It can be observed that SLFB was partially segregated (a segregated zone of 5 mm glass beads at the bottom and a small mixed zone above it) for equal mass combination of 40 gm each (Figure 6). However, for unequal mass combination (Figure 7) the bed was observed to be completely mixed. CFD simulation can also predict comparable configurations of solid and liquid volume fractions compared to experiments.

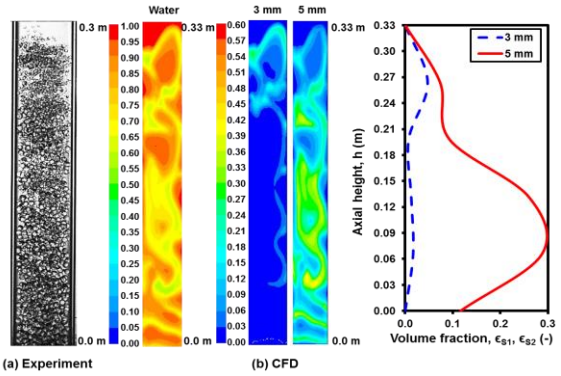

Figure 7: Binary SLFB of 3 mm (40 gm) and 5 mm (240 gm) glass beads: (a) experiment, (b) CFD contours of liquid and solid concentration.

CONCLUSION

In this study, bed expansion behaviour of the binary SLFB system was studied both experimentally and numerically. The findings of the study are summarised below:

- A complete segregation of the bed was observed for both equal and unequal mass ratio of 3 & 8 mm solid particles (8 mm at the bottom & 3 mm at the top).
- The bed was observed to be partially segregated (a segregated zone of 8 mm at the bottom and a mixed zone at the top) for both equal and unequal mass combinations of 5 & 8 mm solid particles.
- For equal solid mass case (40 gm each), the bed was observed to be partially segregated (a segregated zone of 5 mm glass beads at the bottom and a small mixed zone of 3 & 5 mm solid particles above it). However, for unequal mass combination, the bed was observed to be completely mixed.

All the above noted trends were fairly well predicted by the CFD model developed in this study. The CFD predicted bed expansion behaviour shows reasonable agreement (±1-16%) with the experimental results of Khan et al. (2015).

REFERENCES

ANSYS FLUENT Theory Guide. January 2013.

CHENG Y. and ZHU J., (2005), "CFD modeling and simulation of hydrodynamics in liquid-solid circulating fluidized beds", *Can. J. Chem. Eng*., **83** (2), 177-185.

CORNELISSEN J.T., TAGHIPOUR F., ESCUDIE R., ELLIS N. and GRACE J.R., (2007), "CFD modeling of liquid-solid fluidized bed", *Chem. Eng. Sci.*, **62** (22), 6334-6348.

CHAPMAN S. and COWLING, T.G., (1970), "The Mathematical Theory of Non-Uniform Gases", *Third ed. Cambridge University Press*, Cambridge.

CHENG Y. and ZHU, J., (2005), "CFD modeling and simulation of hydrodynamics in liquid-solid circulating fluidized beds", *Can. J. Chem. Eng*., **83** (2), 177-185.

DING J. and GIDASPOW D., (1990), A bubbling fluidization model using kinetic theory of granular flow, *A.I.Ch.E. J.*, **36**, 523-538.

DAVARNEJAD R., ESHGHIPOUR R., ABDI, J. and DEHKORDI, F.B., (2014), CFD Modeling of a Binary Liquid-Solid Fluidized Bed, *Middle-East J. Sci. Res*., **19** (10), 1272-1279.

DOROODCHI E., GALVIN K.P. and FLETCHER, D.F., (2005), "The influence of inclined plates on expansion behaviour of solid suspensions in a liquid fluidized bed—a computational fluid dynamics study", *Powder Tech.*, **156**, 1–7.

ERGUN S., (1952), Fluid Flow through Packed Columns, *Chem. Eng. Prog*., **48**(2), 89-94.

FAN L., GRACE J. and EPSTEIN, N., (2010), "CFD Simulation of a Liquid-Fluidized Bed of Binary Particles", *13th International Conference on Fluidization - New Paradigm in Fluidization Engineering*, Art. 99.

GIDASPOW D., (1994), "Multiphase Flow and Fluidization: Continuum and Kinetic Theory Descriptions", *Academic Press*, Boston, USA.

GIDASPOW D., BEZBURUAH R. and DING J., (1992), "Hydrodynamics of circulating fluidized beds, kinetic theory approach. In: Proceedings of the Seventh Engineering Foundation Conference on Fluidization", *Fluidization*, **7**, 75–82.

IHME F., SCHMIDT-TRAUB, H. and BRAUER H., (1972), "Theoretical studies on mass transfer at and flow past spheres", *Chemie-Ing.-Tech*., **44**(5), 306–313.

JOSHI J.B., (1983), "Solid–liquid fluidized beds: some design aspects", *Chem. Eng. Res. Des*., **61**, 143–161.

KHAN M.S., MITRA S., GHATAGE S.V., PENG Z., DOROODCHI E., MOGHTADERI B., JOSHI J.B., and EVANS G.M., (2015), "Expansion behavior of binary solid-liquid fluidised bed with different solid mass ratio", *APCChE Congress incorporating Chemeca*, Melbourne, Australia, September 27-October 01.

LETTIERI, P., DI FELICE, R., PACCIANI, R. and OWOYEMI, O., (2006), "CFD modeling of liquid fluidized beds in slugging mode", *Powder Tech.*, **167** (2), 94-103.

LUN C., SAVAGE S.B., JEFFSEY D.J., and CHEPURNIY N., (1984), "Kinetic Theories for Granular Flow: Inelastic Particles in Couette Flow and Slightly Inelastic Particles in a General Flow Field", *J. Fluid Mech*., **140**, 223-256.

OGAWA S., UMEMURA A. and OSHIMA, N., (1980), "On the equations of fully fluidized granular materials", *J. App. Math. Phy*., **31**, 483-493.

PANDIT A.B. and JOSHI J.B. (1998), "Pressure drop in packed, expanded and fluidized beds", packed columns and static mixers - a unified approach", *Rev. Chem. Eng.*, **14**, 321–371.

REDDY R.K. and JOSHI J.B., (2009), "CFD modeling of solid–liquid fluidized beds of mono and binary particle mixtures", *Chem. Eng. Sci*., **64** (16), 3641-3658.

REDDY R.K. and JOSHI, J.B., (2007), "CFD modeling of pressure drop and drag coefficient in fixed and expanded beds", *Chem. Eng. Res. Des*. **86**, 444-453.

ROY S. and DUDUKOVIC M.P., (2001), "Flow mapping and modelling of liquid–solid risers", *Ind. Eng. Chem. Res.*, **40**, 5440–5454.

SYAMLAL M., and O'BRIEN, T.J., (1988), "Simulation of granular layer inversion in liquid fluidized beds", *Int. J. Multiphase Flow*, **14**(4), 473-481.

RICHARDSON J.F. and ZAKI W.N., (1954), "Sedimentation and fluidization: part I", *Trans. Ins. Chem. Eng*., **75**, S82-S100.

WEN C.Y. and YU Y.H., (1966), "A generalized method for predicting the minimum fluidization velocity", *AIChE J*., **12** (3), 610-612.